Turbulence-Driven Bootstrap Current in Low-Collisionality Tokamaks

C. J. McDevitt,* Xian-Zhu Tang,† and Zehua Guo‡

Theoretical Division, Los Alamos National Laboratory, Los Alamos, New Mexico 87545, USA

(Received 25 June 2013; published 13 November 2013)

Neoclassical bootstrap current is expected to provide a significant fraction of the equilibrium plasma current in tokamak reactors. Here we report a novel mechanism through which a bootstrap current may be driven even in a collisionless plasma. In analogy with the neoclassical mechanism, in which the collisional equilibrium established between trapped and passing electrons produces a steady state current, we show that resonant scattering of electrons by drift wave microturbulence provides an additional means of determining the equilibrium between trapped and passing electrons and thus driving a bootstrap current. Employing a linearized Fokker-Planck collision operator, the plasma current in the presence of both collisions and resonant electron scattering is computed, allowing for the relative strength of these two mechanisms to be quantified as a function of collisionality and fluctuation amplitude.

DOI: 10.1103/PhysRevLett.111.205002 PACS numbers: 52.55.−s, 52.35.Kt, 52.35.Ra

Neoclassical and turbulent transport can have complex interactions in toroidal confinement devices. For example, turbulent fluctuations can modify neoclassical transport coefficients [1–3]. Here we show that turbulence can significantly modify the bootstrap current, which is conventionally attributed to neoclassical transport [4–7]. We find that the change in bootstrap current is particularly strong during transient bursts of turbulent transport where fluctuation levels can obtain values a few times greater than that estimated from mixing length theory for a steady-state ITER-like tokamak. This suggests that bursty turbulent transport can change the plasma equilibrium and its micro- and macrostability not only through profile relaxation of density and temperature, but also through direct modification of the axisymmetric plasma current distribution via turbulence-induced electron detrapping.

The physical origin of the bootstrap current [8–10] can be understood by a consideration of the guiding center orbits of electrons in a strongly magnetized toroidal confinement device. Namely, in a toroidal plasma, the motion of trapped electrons in the presence of density or temperature gradients results in an asymmetry of comoving versus countermoving trapped electrons. Within the conventional bootstrap current calculation, this trapped electron asymmetry is subsequently translated into a *passing* electron current via the collisional detrapping of electrons. Within this Letter, we describe the means through which an equilibrium between trapped and passing electrons may be established even in the absence of collisions. This observation can be motivated by considering the form of the quasilinear diffusion equation, which may be written as [11,12]

$$\frac{\partial f}{\partial t} = \frac{\partial}{\partial \mathbf{Z}} \cdot \left(\mathbf{D} \cdot \frac{\partial f}{\partial \mathbf{Z}} \right). \tag{1}$$

Here, $\mathbf{D}$ is a 3×3 matrix, and the phase space coordinates for a small inverse aspect ratio plasma may be taken to be $\mathbf{Z} = (v, \lambda, r)$, where v is the magnitude of the velocity, $\lambda \equiv v_\perp^2 B_0/(v^2 B)$ is the pitch angle, and r is the radius. Considering a plot of the location of the trapped-passing boundary as a function of λ and r (see Fig. 1), it is clear that wave-particle interactions provide two distinct mechanisms for detrapping electrons: (i) pitch-angle scattering at a fixed radial location, (ii) radial transport at a fixed location in velocity space. The former process is closely analogous to the familiar collisional detrapping mechanism, except with wave-particle resonances providing the scattering mechanism. With regard to the latter process, for a radially varying equilibrium magnetic field, the location of the trapped-passing boundary will also vary as the electron is transported radially, thus allowing for electrons to be trapped or detrapped via radial scattering. This latter process is likely to be particularly robust, since a broad range of tokamak instabilities introduce substantial amounts of radial transport.

In the following, an explicit form of the quasilinear diffusion equation will be derived for the important case of electrostatic collisionless trapped electron modes [13].

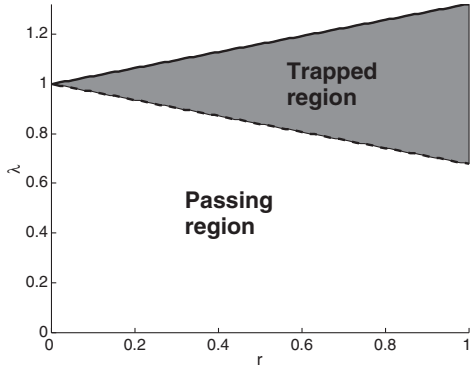

FIG. 1. Trapped particle domain as a function of pitch angle and radius. Detrapping may occur either by pitch-angle scattering or radial transport.

Here, it is shown that the magnetic drift resonance provides an efficient means of detrapping electrons, and thus establishing a collisionless equilibrium between the trapped and passing electron population. The relative efficiency of this collisionless mechanism is subsequently quantified by employing a linearized Fokker-Planck collision operator [14] to provide a description of the steady state electron current in the presence of both Coulomb collisions and resonant electron scattering by collisionless trapped electron modes fluctuations.

The collisionless mechanism for driving bootstrap current by wave-particle interaction can be illustrated by solving the gyrokinetic equation [15]

$$\frac{\partial F_e}{\partial t} + \dot{\mathbf{X}} \cdot \frac{\partial F_e}{\partial \mathbf{x}} + \dot{v}_\parallel \frac{\partial F_e}{\partial v_\parallel} = C_e(F_e). \tag{2}$$

To disentangle mean and fluctuating components of the plasma distribution function, we adopt the standard separation $F_e(\mathbf{z}, t) = \overline{F_e(\mathbf{z})} + \delta F_e(\mathbf{z}, t)$, where $\mathbf{z} \equiv (\mathbf{x}, v_\parallel, \mu)$, $\mu \equiv v_\perp^2/(2B)$, and we will refer to the time independent, axisymmetric, term as the mean component, whereas the second contribution describes fluctuations associated with the background microturbulence. An expression for the mean field can then be written as

$$(v_\parallel \hat{b} + \mathbf{v}_{de}) \cdot \frac{\partial \overline{F}_e}{\partial \mathbf{x}} = C_e(\overline{F_e}) + C_e^{\mathrm{turb}}(\delta F_e), \tag{3}$$

where we have neglected the parallel inductive electric field, made the variable change $(\mathbf{x}, v_\parallel, \mu) \rightarrow (\mathbf{x}, v^2, \mu)$, and the magnetic drift is given by $\mathbf{v}_{de} \equiv -[\mu B(\hat{b} \times \nabla \ln B) + v_\parallel^2(\nabla \times \hat{b})]/|\omega_{ce}|$, with the electron cyclotron frequency $\omega_{ce} \equiv eB/(m_e c)$. Here the turbulent collision operator is defined as

$$\frac{B}{v_\parallel} C_e^{\mathrm{turb}}(\delta F_e) = -\frac{\partial}{\partial \mathbf{x}} \cdot \mathbf{\Gamma}_x - \frac{\partial}{\partial v^2}\bigg|_\mu \Gamma_{v^2}, \tag{4}$$

with the radial and velocity space fluxes given by

$$\mathbf{\Gamma}_x \equiv \overline{\dot{\mathbf{X}} \frac{B}{v_\parallel} \delta F_e}, \qquad \Gamma_{v^2} \equiv 2\overline{\frac{e}{m_e} \mathbf{v}_{de} \cdot \nabla \delta\phi \frac{B}{v_\parallel} \delta F_e}. \tag{5}$$

For simplicity, we have assumed the limit of tightly localized radial eigenmodes [16] such that $k_\parallel \approx 0$. The mechanism described here can thus be distinguished from that described by Wang *et al.* [17] (see also Itoh and Itoh [18]), which requires $\langle k_\parallel \rangle \sim \sum_k k_\parallel |\delta\phi_k|^2 \neq 0$, and Hinton *et al.* [2], which arose primarily due to magnetic flutter. Expanding the mean component of the distribution function in the ratio of the poloidal Larmor radius over an equilibrium scale length, i.e., $\overline{F_e} = \overline{F_{e0}} + \overline{F_{e1}} + \cdots$, yields to lowest nontrivial order

$$\mathbf{B} \cdot \nabla \left[\overline{F_{e1}} - v_\parallel \frac{I(\psi)}{|\omega_{ce}|} \frac{\partial \overline{F_{e0}}}{\partial \psi} \right] = \frac{B}{v_\parallel} [C_e^{\mathrm{turb}}(\delta F_e) + C_e(\overline{F_{e1}})], \tag{6}$$

where ψ is the poloidal flux function. Our primary focus is the reactor-relevant regime where both the collisional and resonant electron scattering rates are slow compared to the bounce time of a trapped electron. This allows the right-hand side of Eq. (6) to be treated as a perturbation. Introducing the additional expansion $\overline{F_{e1}} = F_{e1}^{(0)} + F_{e1}^{(1)} + \cdots$, the lowest order solution is given by [19]

$$F_{e1}^{(0)} = v_\parallel \frac{I(\psi)}{|\omega_{ce}|} \frac{\partial \overline{F_{e0}}}{\partial \psi} + H_e, \tag{7}$$

where $H_e = H_e(\psi, v^2, \mu, \sigma)$ is an integration constant and $\sigma \equiv v_\parallel/|v_\parallel|$. The integration constant H_e will be determined by the next order equation

$$\mathbf{B} \cdot \nabla F_{e1}^{(1)} = \frac{B}{v_\parallel} [C_e^{\mathrm{turb}}(\delta F_e) + C_e(F_{e1}^{(0)})]. \tag{8}$$

For trapped electrons, it can be straightforwardly demonstrated that the odd component of H_e vanishes identically [6]. For passing electrons, a formal expression for $H_e(\psi)$ may be obtained by flux surface averaging Eq. (8), yielding

$$\left\langle \frac{B}{v_\parallel} [C_e^{\mathrm{turb}}(\delta F_e) + C_e(F_{e1}^{(0)})] \right\rangle = 0. \tag{9}$$

Equation (9) provides a constraint equation for the mean electron distribution incorporating both Coulomb collisions and resonant scattering of electrons by drift wave turbulence. This constraint equation, in conjunction with the boundary condition $H_e^{\mathrm{odd}} = 0$ at the trapped-passing boundary, will be used in the following to describe the mean electron current.

The strength of the resonant scattering contribution may be estimated by evaluating the turbulent collision operator [Eq. (4)] from quasilinear theory. The linearized drift kinetic equation for electrons can be written as

$$\left[\frac{\partial}{\partial t} + (v_\parallel \hat{b} + \mathbf{v}_{de}) \cdot \nabla + \Delta\omega \right] \delta F_e = -\frac{c}{B_\parallel^*} (\hat{b} \times \nabla \delta\phi) \cdot \frac{\partial \overline{F_e}}{\partial \mathbf{x}} - 2\frac{e}{m_e} \mathbf{v}_{de} \cdot \nabla \delta\phi \frac{\partial \overline{F_e}}{\partial v^2}\bigg|_\mu, \tag{10}$$

where $\Delta\omega$ is a small resonance broadening term. Collisionless trapped electron modes satisfy the ordering $\omega_b \gg (\omega, \omega_{de}) \gg \nu_{\mathrm{eff}}$, such that the collision operator may be neglected in Eq. (10). Here ω_b is the bounce frequency of a thermal electron, ω_{de} the electron magnetic drift frequency, $\nu_{\mathrm{eff}} \equiv \nu_e/\varepsilon$ and $\varepsilon \equiv r/R_0$. Equation (10) may be inverted by utilizing the scale separation $(\omega, \omega_{de}) \ll \omega_b$, which allows for an approximate analytic inversion [20]. For the bootstrap current calculation, while

the scale separation $(\omega, \omega_{de}) \ll \omega_b$ should be satisfied throughout the majority of phase space, it is expected to break down near the trapped-passing boundary where $\omega_b \to 0$. To overcome this difficulty with the approximate analytic inversion, we employ a direct numerical inversion when computing the quasilinear fluxes. After performing the variable change $(\mathbf{x}, v^2, \mu) \to (\mathbf{x}, v, \kappa)$, the turbulent collision operator may be written as

$$\langle \mathcal{J} C_e^{\rm turb} \rangle = \frac{-1}{V'} \frac{\partial}{\partial \psi} V' \langle \Gamma_x \rangle - \frac{\partial}{\partial v} \langle \Gamma_v \rangle - \frac{\partial}{\partial \kappa} \langle \Gamma_\kappa \rangle, \quad (11)$$

where, after inverting the drift kinetic equation, the phase space fluxes can be shown to have the form

$$\begin{pmatrix} \langle \Gamma_\kappa \rangle \\ \langle \Gamma_v \rangle \\ \langle \Gamma_x \rangle \end{pmatrix} = - \begin{pmatrix} D_{\kappa\kappa} & D_{\kappa v} & D_{\kappa x} \\ D_{v\kappa} & D_{vv} & D_{vx} \\ D_{x\kappa} & D_{xv} & D_{xx} \end{pmatrix} \begin{pmatrix} \frac{\partial H_e}{\partial \kappa} \\ \frac{\partial H_e}{\partial v} \\ \frac{\partial H_e}{\partial \psi} \end{pmatrix} + \begin{pmatrix} S_\kappa \\ S_v \\ S_x \end{pmatrix},$$

and the Jacobian is given by $\mathcal{J} = 2\pi\varepsilon\kappa(v/v^{\rm the})^3 \lambda^2 (B/B_0)(v^{\rm the}/v_\parallel)$. Here κ is a pitch-angle variable defined by $\kappa \equiv \sqrt{[1 - \lambda(1-\varepsilon)]/(2\varepsilon\lambda)}$, $\lambda \equiv 2\mu B_0/v^2$, and the spatial and velocity derivatives transform as

$$\left.\frac{\partial}{\partial \mathbf{x}}\right|_{\mu, v^2} = \left.\frac{\partial}{\partial \mathbf{x}}\right|_{v,\kappa} + \left(\frac{1/2 - \kappa^2}{2\kappa}\right) \frac{\partial \ln \varepsilon}{\partial \mathbf{x}} \left.\frac{\partial}{\partial \kappa}\right|_{x,v},$$

$$\left.\frac{\partial}{\partial v^2}\right|_{x,\mu} = \frac{1}{2v} \left.\frac{\partial}{\partial v}\right|_{x,\kappa} + \frac{1 - \varepsilon + 2\varepsilon\kappa^2}{4\varepsilon\kappa v^2} \left.\frac{\partial}{\partial \kappa}\right|_{x,v}.$$

The variable κ has a range given by $(0, \infty)$, where the trapped-passing boundary corresponds to $\kappa = 1$. Electrons with $\kappa > 1$ are passing, whereas those with $0 < \kappa < 1$ are trapped. The contributions to the flux given by S_κ, S_v, and S_x are proportional to the thermodynamic forces and provide the drive for $H_e^{\rm odd}$. A distinctive characteristic of the turbulent collision operator is that when performing the change of variables $(v^2, \mu) \to (v, \kappa)$, the spatial derivative at fixed (μ, v^2) is linked to *both* spatial and pitch-angle gradients. This has the important consequence that electrons may be detrapped via radial transport at fixed locations in velocity space, in addition to the more familiar pitch-angle scattering mechanism. As an example of the phase space structure of the quasilinear transport coefficients, the pitch-angle diffusivity is plotted in Fig. 2. The pitch-angle diffusivity can be seen to be maximal near the trapped-passing boundary, suggesting that resonant scattering provides a robust means of detrapping electrons.

Before solving for the plasma current in the presence of both Coulomb collisions and resonant electron scattering, it will be useful to consider the collisionless limit $\nu_e^* \to 0$, where the dimensionless collisionality is defined by $\nu_e^* \equiv (qR_0/\sqrt{2}v^{\rm the})\varepsilon^{-3/2}\tau_{ee}^{-1}$ and $v^{\rm the} \equiv \sqrt{T_e/m_e}$. Our motivation for considering this idealized limit is that it provides an unambiguous demonstration that resonant electron scattering may drive a mean electron current in the absence of collisions. Subsequently, the case of finite collisionality will be considered in order to quantify the impact of resonant electron scattering on the plasma current as a function of ν_e^* and fluctuation amplitude.

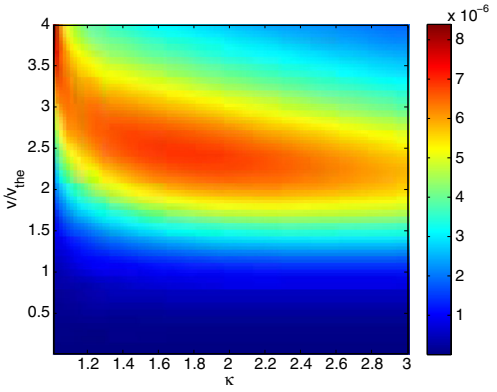

FIG. 2 (color online). Plot of the diffusivity $aD_{\kappa\kappa}/v^{\rm the}$ at $r/a = 0.55$ in the passing particle region for the parameters $\rho_* = 1/250$, $\varepsilon_{\rm max} = 0.32$, $L_n^{\rm max}/a = 1.0$, $L_{Te}^{\rm max}/a = 0.5$, $q_0 = 3.0$, $T_e = T_i$, $\sqrt{m_i/m_e} \approx 60$, and $a\Delta\omega/c_s = 0.2$. We assumed five modes to be present with wave numbers between $k_\theta \rho_i = 0.25$–1.0, where the fluctuation spectrum is defined by Eq. (12) below.

The solution of the constraint equation (9) in the collisionless limit is shown in Fig. 3, with the resulting current profile shown by the black curve in Fig. 4. Here, we have assumed the magnetic geometry to be described by unshifted circular flux surfaces with a constant flux function $I(\psi) = B_0 R_0$, $H_e^{\rm odd}$ is assumed to vanish as $v \to \infty$ as well as at $v = 0$, and we have also enforced $\partial H_e/\partial\kappa \to 0$ as $\kappa \to \infty$. For simplicity, we have assumed a no-slip boundary condition in the radial direction. The density and temperature profiles were assumed to be of the form

$$\left[\frac{n_e(r)}{n_e(a)}, \frac{T_e(r)}{T_e(a)}\right] = 1 - e^{-L} + e^{L\cos(\pi\Delta r/L) - \delta(\Delta r - L)\pi},$$

where $L \equiv (r_{\rm max} - r_{\rm min})/\pi L_{n,T_e}^{\rm max}$, $\Delta r \equiv (r - r_{\rm min})/\pi L_{n,T_e}^{\rm max}$ and $L_{n,T_e}^{\rm max}$ refers to either the maximum density or

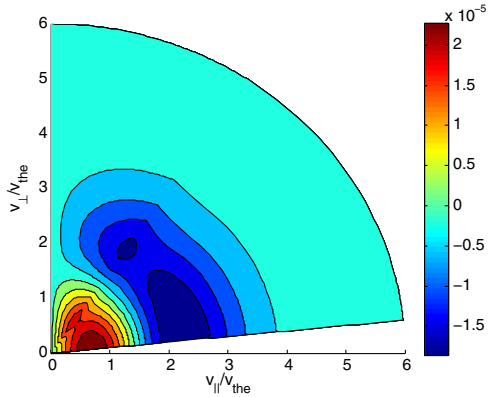

FIG. 3 (color online). Plot of $F_{e1}^{(0)}$ at $r/a = 0.55$ for the same parameters as Fig. 2.

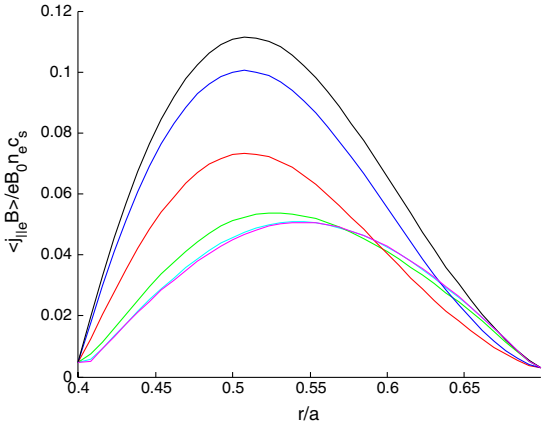

FIG. 4 (color online). The radial profile of the electron current for: no turbulence (magenta line), $\nu_e^* = 10^{-1}$ (cyan line), $\nu_e^* = 10^{-2}$ (green line), $\nu_e^* = 10^{-3}$ (red line), $\nu_e^* = 10^{-4}$ (blue line), and $\nu_e^* = 0$ (black line). The amplitude of the turbulent fluctuations was assumed to be $\langle |e\delta\phi/T| \rangle \approx 5 \times 10^{-3}$.

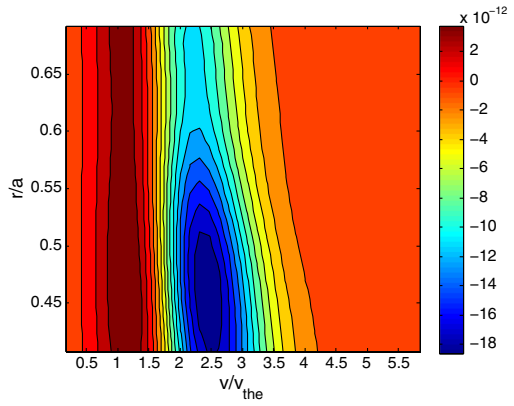

FIG. 5 (color online). Plot of the pitch-angle flux $\Gamma_\kappa^{(\kappa)}$ at the trapped-passing boundary neighboring the $v_\parallel > 0$ region. Positive values indicate detrapping of electrons, whereas negative values indicate electron trapping.

temperature gradient. The profile of the safety factor will also be taken to have the form $q(r) = q_0(r/a)^{1/2}$.

In order to better understand the physical origin of the electron current discussed above, it will be useful to consider the flux of electrons through the trapped-passing boundary. A contour plot of this flux is shown in Fig. 5 for the trapped-passing boundary bordering the positive passing particle region. From Fig. 5, a clear imbalance in both the rate as well as energy of electron trapping versus detrapping can be observed. Since we are considering the odd component of the electron distribution function, this trend would be reversed for the flux through the trapped-passing boundary neighboring the negative passing particle region. This asymmetry between the trapping or detrapping rate for the positive and negative passing particle regions will thus lead to a deficit of electrons propagating in the positive direction, and thus a positive net passing electron current. At stationarity, this current drive mechanism is balanced by a radial flux of electron momentum out of the simulation domain, yielding a peaked electron current profile such as that shown in Fig. 4.

Turning now to the more general case where both Coulomb collisions and resonant electron scattering are included, it is useful to estimate the relative strength of these two mechanisms. Considering the pitch-angle diffusion coefficient as a representative example, a straightforward calculation yields

$$\frac{D_\kappa^{QL}}{D_\kappa^{\mathrm{neo}}} \sim \sqrt{\frac{m_e}{m_i}}\left(\frac{q}{\varepsilon^{5/2}}\right)\left(\frac{L_n}{R_0}\right)\left(\frac{v}{v^{\mathrm{the}}}\right)^3 \frac{1}{\nu_e^*}\left|\frac{e\delta\phi_k}{T}\right|^2,$$

where we have considered the region near the trapped-passing boundary where $v_\parallel/v \sim \sqrt{\varepsilon}$ and $\kappa \approx 1$. From the above scaling it is evident that while Coulomb collisions are likely to be dominant at low energies, resonant scattering becomes increasingly important at high energies. This is of particular importance when noting that the detrapping flux of electrons is maximal in the energy range $v/v^{\mathrm{the}} = 2$–3.5 (see Fig. 5), allowing for a robust contribution from resonant electron scattering in this region.

In order to carry out a more comprehensive estimate of the relative strength of the turbulent and collisional contributions, it will be necessary to introduce an explicit model of the turbulence spectrum. The turbulence spectrum will be modeled following assumptions similar to those made in the quasilinear transport code QUALIKIZ [21]. In particular, we will assume a peaked turbulence spectrum of the form

$$|\delta\phi_k|^2 \sim \exp(4k_\theta\rho_i - 8k_\theta^{\max}\rho_i), \tag{12a}$$

for $k_\theta < k_\theta^{\max}$, where $k_\theta^{\max}$ indicates the wave number of the most unstable mode, and

$$|\delta\phi_k|^2 \sim \exp(-4k_\theta\rho_i), \tag{12b}$$

for $k_\theta > k_\theta^{\max}$. With the above assumptions, a plot of the radial profile of the plasma current for multiple values of ν_e^* is shown in Fig. 4. We note that in the absence of turbulence, for $\nu_e^* \ll 1$, the current profile is anticipated to be insensitive to ν_e^* according to neoclassical theory. Here, in contrast, a clear dependence of the current profile on ν_e^* is present until the system asymptotes to its collisionless value. Similarly, a plot of the current profile as a function of turbulence intensity is shown in Fig. 6 for an ITER relevant collisionality [22,23] of $\nu_e^* = 2 \times 10^{-3}$ and $\rho^* = 10^{-3}$. We note that the resultant current profile is highly sensitive to the turbulent fluctuation level, making a precise quantification of the strength of the turbulent mechanism problematic for ITER plasmas. Further complicating a detailed estimate of the strength of the turbulent mechanism is the observation that flux driven turbulent systems are typically characterized by bursty, intermittent

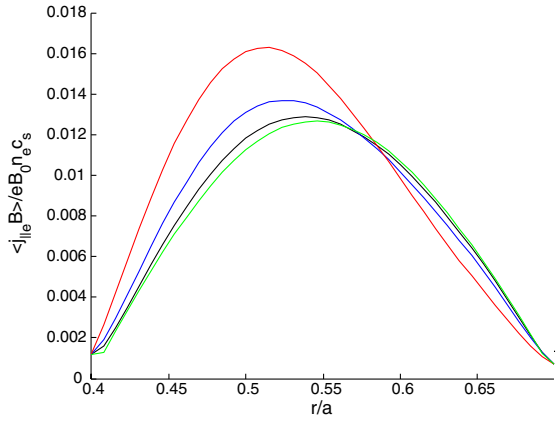

FIG. 6 (color online). The radial profile of the electron current for: no turbulence (green line), $\langle|e\delta\phi/T|\rangle \approx 1.25 \times 10^{-3}$ (black line), $\langle|e\delta\phi/T|\rangle \approx 2.5 \times 10^{-3}$ (blue line), and $\langle|e\delta\phi/T|\rangle \approx 5 \times 10^{-3}$ (red line). The collisionality was taken to be $\nu_e^* = 2 \times 10^{-3}$.

transport events, such that the fluctuation level may transiently rise well above its ambient level [24–26]. It is, however, clear that for fluctuation levels in excess of $\langle|e\delta\phi/T|\rangle \approx 2.5 \times 10^{-3}$, significant modifications to the electron current profile are expected.

In summary, we have uncovered an effective means through which turbulence may impact the mean electron current. This turbulent effect arises through a direct modification of the bootstrap current (as opposed to bootstrap current modification through profile relaxation), and thus provides a novel channel through which turbulence may modify plasma macrostability. A particularly subtle physics is how radial transport by turbulence can provide effective detrapping of the electrons due to the changing trapped-passing boundary on different flux surfaces.This provides a robust coupling between anomalous transport and bootstrap current drive. Future work will focus on understanding how modifications to the bootstrap current arising from large transient events will impact the macrodynamics of the magnetohydrodynamic equilibrium.

We wish to thank Allen Boozer, Patrick Diamond, Taik Soo Hahm, Per Helander, Felix Parra, Ron Waltz, and Weixing Wang for useful discussions. This work was supported by Department of Energy Office of Fusion Energy Sciences for support under Contract No. DE-AC52-06NA25396.

*mcdevitt@lanl.gov
†xtang@lanl.gov
‡guo@lanl.gov

[1] H. Biglari and P. H. Diamond, Phys. Fluids B **5**, 3838 (1993).
[2] F. L. Hinton, R. E. Waltz, and J. Candy, Phys. Plasmas **11**, 2433 (2004).
[3] H. E. Mynick and A. H. Boozer, Phys. Plasmas **12**, 062513 (2005).
[4] R. J. Bickerton, J. W. Connor, and J. B. Taylor, Nature (London) Phys. Sci. **229**, 110 (1971).
[5] A. A. Galeev, Zh. Eksp. Teor. Fiz. **59**, 1378 (1971) [Sov. Phys. JETP **32**, 752 (1971)].
[6] F. L. Hinton and R. D. Hazeltine, Rev. Mod. Phys. **48**, 239 (1976).
[7] S. P. Hirshman and D. J. Sigmar, Nucl. Fusion **21**, 1079 (1981).
[8] W. A. Houlberg, K. C. Shaing, S. P. Hirshman, and M. C. Zarnstorff, Phys. Plasmas **4**, 3230 (1997).
[9] W. X. Wang, G. Rewoldt, W. M. Tang, F. L. Hinton, J. Manickam, L. E. Zakharov, R. B. White, and S. Kaye, Phys. Plasmas **13**, 082501 (2006).
[10] E. A. Belli and J. Candy, Plasma Phys. Controlled Fusion **54**, 015015 (2012).
[11] A. N. Kaufman, Phys. Fluids **15**, 1063 (1972).
[12] A. J. Brizard and A. A. Chan, Phys. Plasmas **11**, 4220 (2004).
[13] J. C. Adam, W. M. Tang, and P. H. Rutherford, Phys. Fluids **19**, 561 (1976).
[14] P. J. Catto and K. T. Tsang, Phys. Fluids **20**, 396 (1977).
[15] A. J. Brizard and T. S. Hahm, Rev. Mod. Phys. **79**, 421 (2007).
[16] T. S. Hahm and W. M. Tang, Phys. Fluids B **3**, 989 (1991).
[17] W. X. Wang, S. Ethier, T. S. Hahm, W. M. Tang, and A. Boozer, in *Proceedings of the 24th IAEA International Conference on Plasma Physics and Controlled Nuclear Fusion Research, San Diego, CA* (IAEA, Vienna, 2012), TH/P7-14.
[18] S. I. Itoh and K. Itoh, Phys. Lett. **127A**, 267 (1988).
[19] P. Helander and D. J. Sigmar, *Collisional Transport in Magnetized Plasmas* (Cambridge University Press, Cambridge, England, 2002).
[20] F. Y. Gang and P. H. Diamond, Phys. Fluids B **2**, 2976 (1990).
[21] C. Bourdelle, X. Garbet, F. Imbeaux, A. Casati, N. Dubuit, R. Guirlet, and T. Parisot, Phys. Plasmas **14**, 112501 (2007).
[22] C. Gormezano *et al.*, Nucl. Fusion **47**, S285 (2007).
[23] E. J. Doyle *et al.*, Nucl. Fusion **47**, S18 (2007).
[24] D. E. Newman, B. A. Carreras, P. H. Diamond, and T. S. Hahm, Phys. Plasmas **3**, 1858 (1996).
[25] Y. Sarazin, V. Grandgirard, J. Abiteboul, S. Allfrey, X. Garbet, P. Ghendrih, G. Latu, A. Strugarek, and G. Dif-Pradalier, Nucl. Fusion **50**, 054004 (2010).
[26] S. Jolliet and Y. Idomura, Nucl. Fusion **52**, 023026 (2012).